

Combined Eulerian-Lagrangian or Pseudo-Lagrangian Descriptions of Waves Caused by an Advancing Free Surface Disturbance

Hong Gun Sung¹ and Stéphan T. Grilli²

¹ Maritime & Ocean Engineering Research Institute (MOERI, former KRISO), Korea Ocean Research & Development Institute, Daejeon, Korea

² Department of Ocean Engineering, University of Rhode Island, Narragansett RI, USA

ABSTRACT

We develop a new methodology for the numerical modeling of nonlinear free surface waves, caused by an advancing free surface disturbance, based on combining Lagrangian and Eulerian, or pseudo-Lagrangian, methods for the time updating of free surface geometry and motion. We solve potential flow equations with a three-dimensional (3D) higher-order Boundary Element Method (BEM; Grilli et al., 2000, 2001; and Sung and Grilli, 2005, for some more recent extensions).

Specifically, the Lagrangian and Eulerian methods are combined in order to exploit their respective advantages. The full Lagrangian updating is very accurate for highly nonlinear waves, and the Eulerian or pseudo-Lagrangian methods yield smaller computational times because they allow using a shorter domain, particularly for the forward speed problem of an advancing disturbance on or below the free surface. As a validation application, we compute 3D nonlinear waves caused by a moving pressure patch. Numerical results show that the present methodology works quite well and gives reasonable wave resistance for numerical examples, as compared with theory, and other computations based on full Lagrangian and pseudo-Lagrangian methods.

KEY WORDS: Numerical modeling of free surface flows, advancing disturbance, combination of Lagrangian and Eulerian description, boundary element method (BEM), nonlinear pressure patch problem.

INTRODUCTION

Within the realm of linear potential flow theory, an advancing disturbance on or below the free surface creates a so-called Kelvin wave pattern, that is well described in the classical literature. However, free surface waves created by high-speed moving disturbances, such as a Surface Effect Ship (SES), may be strongly nonlinear and hence greatly differ from the linear wave field. Thus, it is necessary to tackle this problem through numerical modeling.

The history of wave analysis around moving ships can be traced back to Michell, Havelock, Wehausen, and other precursors of naval hydrodynamics. Most of these classical works deal with some

aspects of and definition of “wave resistance,” or the theoretical prediction of wave resistance of simple bodies or ship hulls having simplified analytic lines (Wehausen, 1973). A review of analytical representations of ship waves can be found in Noblesse (2000).

When it comes to numerical computations for wave resistance, the Boundary Element Method (BEM), also originally referred to as “panel method”, has been widely used since the pioneering works of Hess and Smith (1964) and Dawson (1977). In the present work, we briefly review the state-of-the-art in computational methods for ship wave resistance problem and make some recommendations for new developments, in light of our past experience with three-dimensional (3D) BEM computations of nonlinear free surface flows (e.g., Grilli et al., 2000, 2001). Specifically in the present work, we confine our focus to the problem of the time updating algorithm for the free surface geometry and motion.

Although some other methods based on a direct solution of Navier-Stokes equations have been recently proposed, mostly to address the problem of friction resistance of a ship hull, potential flow theory is still the most widely used and accurate formalism for solving the ship wave resistance problem. Wave resistance for a constant forward speed has usually been formulated as a steady wave flow problem in a reference frame moving with the ship. As pointed out in Sclavounos et al. (1997), the steady flow not only yields wave resistance, but also sinkage and trim, which are significant factors in determining power requirements and operating condition of the ship hull. Following initially mostly analytical methods, more practical and quantitative results were obtained through numerical modeling. By the late 1970’s, the so-called Neumann-Kelvin (NK) approach was beginning to be used in predicting zero or non-zero forward speed problems. In the NK approach, the body boundary condition is applied on the mean position of the exact body surface with the linearized free surface boundary conditions. As indicated in Beck and Reed (2001), the first practical application of NK based on a BEM can be attributed to Hess and Smith (1964). [Note that many research papers refer to the BEM as a “panel method” because a piecewise constant or linear quadrilateral approximation of geometry and field functions have initially been more widely used in numerical computations.]

A further refinement was to use the exact hull boundary condition but still with linearized free surface boundary conditions. This approach did not gain popularity, and Dawson (1977) devised the

“double-body” or “Dawson’s approach,” by linearizing about the double-body flow. An improvement of Dawson’s approach is the weak-scatter hypothesis of Pawloski (1991). The wave disturbance by the ship motion is linearized around the ambient waves with the exact ship hull boundary condition. Huang and Slavounos (1998) utilized this approximation for developing the SWAN4 model.

By contrast, the Fully Nonlinear Potential Flow (FNPF) approach does not require any kind of approximation of the body nor of the free-surface boundary conditions. For the steady forward motion, initial results of using this approach can be found in Jensen et al. (1989), Raven (1998), and Liu et al. (2001). For unsteady ship wave problems, a time marching scheme must be used which, as indicated by Beck and Reed (2001), gives rise to additional difficulties, particularly in the Eulerian-Lagrangian representation. Among these difficulties, the local treatment of the breaking waves generated around the ship bow and stern particularly for high-speed ships is a very important one. To be able to pursue numerical simulations using a FPNF-BEM beyond wave breaking, local absorption of wave energy in regions of the free surface having nearly breaking waves must be implemented. In this respect, some success was reported by Beck (1999) and, more recently, using a spilling breaker model, by Muscari and Di Mascio (2004).

The long term goal of this work deals is the application of an existing 3D-FNPF-BEM model (Grilli and Horrillo, 1997; Grilli et al., 2000, 2001; Fochesato et al., 2005) to the computations of the wave resistance of high speed SES vessels, such as the Harley FastShip, which is a new type of SES with catamaran hulls. Extensions of the model for solving the present problem were initially proposed by Sung and Grilli (2005). In this paper, we introduce a new time updating methodology, for the numerical modeling of free surface waves around an advancing disturbance, by combining Lagrangian and Eulerian (or Pseudo-Lagrangian) descriptions of the free surface.

In the following sections, the mathematical and numerical formulations of the model are presented, with the emphasis on the method of free surface updating. Other aspects of the model are detailed in earlier papers. The problem of nonlinear waves caused by a traveling pressure patch is solved to validate the proposed combined method of free surface updating.

FORMULATION

We assume the fluid to be incompressible, inviscid, and the flow to be irrotational. We thus define a velocity potential, as the scalar function $\Phi(\vec{x}, t)$, of spatial variables, $\vec{x} = (x, y, z) = (x_1, x_2, x_3)$, and time variable t . The velocity potential is related to the fluid velocity vector, $\vec{u} = (u, v, w)$ as,

$$\vec{u} = \nabla\Phi \quad (1)$$

where ∇ denotes the gradient operator. The continuity equation in the fluid domain $\Omega(t)$ becomes a Laplace’s equation for the potential,

$$\nabla^2\Phi(\vec{x}, t) = 0 \quad (2)$$

where, ∇^2 is the Laplacian operator, which is defined as, $\nabla^2 = \nabla \cdot \nabla$.

The boundary of the computational domain is composed of the free surface, body boundary, and far field (downstream or upstream) boundaries. Appropriate boundary conditions must be specified on the entire domain boundary. According to the Lagrangian framework, the kinematic and dynamic free surface conditions are expressed as,

$$\frac{D\vec{R}}{Dt} = \vec{u} \equiv \nabla\Phi \quad (3)$$

$$\frac{D\Phi}{Dt} = -gz + \frac{1}{2}|\nabla\Phi|^2 - \frac{p_a}{\rho} \quad (4)$$

respectively, where $\vec{R} = (X, Y, Z)$ is the free surface position vector, \vec{u} is the Lagrangian velocity of the free surface, g is the gravitational constant, ρ the density of the fluid, p_a the atmospheric or applied pressure on the free surface (e.g., due to the SES air cushions), and $D/Dt = \partial/\partial t + \vec{u} \cdot \nabla$ is the material derivative.

If one assumes a purely Eulerian representation, the same equations are expressed as a function of the free surface elevation: $z = \zeta(x, y, t)$. By taking the material derivative of the kinematic boundary condition, $D/Dt[\zeta(x, y, t) - z] = 0$, we get,

$$\frac{\partial\zeta}{\partial t} = -\nabla_H\Phi \cdot \nabla_H\zeta + \frac{\partial\Phi}{\partial z} \quad (5)$$

where ∇_H denotes the horizontal component of the gradient operator. The corresponding form for the dynamic boundary condition is,

$$\frac{\partial\Phi}{\partial t} = -gz - \frac{1}{2}|\nabla\Phi|^2 - \frac{p_a}{\rho} \quad (6)$$

As stated above, the primary goal of the paper is the numerical time updating of free surface boundary conditions and geometry; hence, we will detail this further in the following sections.

The body boundary condition in the potential fluid flow states that the normal velocity should be continuous from the fluid to the body, as follows.

$$\nabla\Phi \cdot \vec{n} = \vec{V} \cdot \vec{n} \quad (7)$$

where, $\vec{n} = (n_x, n_y, n_z)$ is the unit normal vector pointing outward from the fluid domain, and \vec{V} is the velocity vector of the body at the point of application. Usually, the velocity vector is given by the specified motion of the disturbance, or determined by considering the equations of body motion.

On the sea bottom and other fixed parts of the boundary, a no-flow boundary condition is prescribed as

$$\nabla\Phi \cdot \vec{n} = 0 \quad (8)$$

The boundary conditions specified on the vertical upstream and downstream boundaries are very important for obtaining accurate and reliable numerical results. For the steady translation of a surface vessel or an advancing pressure patch in still water, the far field condition is of the form,

$$\lim_{r \rightarrow \infty} \nabla\Phi = (0, 0, 0) \quad (9)$$

Where r denotes the radial distance from the source of the disturbance. Due to the truncation of the fluid domain, one has to modify the exact far field condition (9) into Eq. (8), i.e., a no-wave condition expressing that waves will be essentially traveling downstream. This can be achieved by specifying $\Phi = 0$ on the truncated radiation boundary. It is noted that all of the above equations are stated in earth-fixed coordinates. In order to improve the numerical efficiency, a reference frame moving with the disturbance is introduced; this was detailed in Sung and Grilli (2005).

Free Surface Time Update Methods

In problems with zero forward speed, the so-called Lagrangian approach of free surface time updating, based on Eqs. (3) and (4), is most often used. An Eulerian description, based on Eqs. (5) and (6), has also been used, particularly for nonlinear wave simulations in which the wave overturning does not occur. The Lagrangian approach is referred to as the material node approach. Its advantage is that the formulation is very straightforward, and it provides information on how the fluid particles move under wave motion. As indicated in Beck (1999), one of the difficult numerical issues with this method is that fluid markers tend to accumulate around stagnation points and regions of relatively high flow speed, which leads to numerical instability problems. One can prevent the failure of the time-marching algorithm

by relocating (or regridding) fluid markers from time to time; this however, is a difficult task. The Lagrangian approach has been used for simulating plunging breakers in deep or shallow water (e.g., Dommermuth et al., 1988; Grilli et al., 1997). By contrast, regridding is not required with the Eulerian method, but we need to numerically evaluate the horizontal gradient of the free surface elevation, to be used in Eq. (5), and the method is limited to single-valued free surface elevations.

For forward speed problems, the Eulerian approach has some advantages over the Lagrangian method for time updating. With the Lagrangian approach, expressed in earth-fixed coordinates, one should generally use a very long computational domain, to get a long enough time history or reach steady-state, in time-domain nonlinear simulations of wave generation by an advancing disturbance. Furthermore, grid resolution must be very dense around the disturbance (or ship) to capture the steeper waves around the bow and stern. Such calculations may be very time-consuming and inefficient for very large, finely discretized, computational domains. A practical solution to this problem is to use a coordinate system moving with the disturbance and adopt an Eulerian or pseudo-Lagrangian updating. This is discussed below.

For forward speed problems in a moving reference frame, the total velocity potential has usually been expressed as the sum of the free-stream velocity potential, which corresponds to the translation of the disturbance, and the perturbed potential, after introducing moving reference frame. For this problem, Beck (1999) suggested a pseudo-Lagrangian approach for free surface updating, which allows the markers to follow a prescribed path. He thus defined a time derivative following the moving nodes as, $\delta / \delta t = \partial / \partial t + \vec{v} \cdot \nabla$ where \vec{v} is the velocity of the moving node (which is different from that of true fluid particles). He finally set $\vec{v} = (0, 0, \partial \zeta / \partial t)$, which forces the markers/free surface nodes to remain at the same horizontal location in the moving reference frame; his final equations reduce to,

$$\frac{\partial \zeta}{\partial t} = -\nabla_H \Phi \cdot \nabla_H \zeta + \frac{\partial \Phi}{\partial z} - U_B(t) \frac{\partial \zeta}{\partial x} \quad (10)$$

$$\frac{\partial \Phi}{\partial t} = -gz - \frac{1}{2} |\nabla \Phi|^2 - \frac{p_a}{\rho} + \frac{\partial \zeta}{\partial t} \frac{\partial \Phi}{\partial z} - U_B(t) \frac{\partial \Phi}{\partial x} \quad (11)$$

where $U_B(t)$ is the forward speed (assumed in x-direction). It is noted that Eqs. (10) and (11), except for the effect of the translation speed, are of the same form as the corresponding equations in Sung et al. (2000), which were developed in an Eulerian framework, such as Eqs. (5) and (6). In this regard, Beck's approach can be viewed as an Eulerian updating method. Beck (1999) also indicated that another appropriate choice of \vec{v} is one that approximates the true fluid velocity reasonably well, but he did not provide any detailed formulation for this numerical algorithm.

Similarly to the conventional approach, Sung and Grilli (2005) proposed a new scheme for free surface updating, in which fictitious fluid particles keep the values of their x-coordinates in the moving reference frame.

$$\frac{\tilde{D}\vec{R}}{\tilde{D}t'} = W_y \vec{e}_y + W_z \vec{e}_z \quad (12)$$

$$\frac{\tilde{D}\Phi}{\tilde{D}t'} = \Phi_{t'} + W_y \frac{\partial \Phi}{\partial y} + W_z \frac{\partial \Phi}{\partial z} \quad (13)$$

where the prime (') denotes the coordinates of the moving reference frame, \vec{e}_y , and \vec{e}_z are the unit vector in y- and z-direction, and the pseudo-Lagrangian velocity is $\vec{W} = (W_x, W_y, W_z)$ with

$$W_x = U_B(t), W_y = \frac{\partial \Phi}{\partial y}, W_z = \frac{\partial \Phi}{\partial z} - \frac{n^x}{n^z} \left[U_B(t) - \frac{\partial \Phi}{\partial x} \right] \quad (14)$$

In this updating scheme, the fictitious fluid markers keep their relative horizontal position (in x only) in the reference frame. Sung and Grilli showed that the proposed method works quite well and provides accurate and efficient results for the nonlinear pressure patch problem.

In summary, for updating the free surface in time, there are three different approaches, the : material node, Eulerian, and pseudo-Lagrangian, approaches. In the following section, we present a new combined time updating method.

Combined Method of Free Surface Time Updating

To exploit their respective advantages, we combine the Lagrangian and Eulerian (or pseudo-Lagrangian) update as follows.

1) We express our equations in the conventional moving reference frame. Thus, the boundary integral equation is solved in the moving reference frame using the 3D-BEM.

2) The wave elevation $\zeta^E(x, y, t)$ is obtained by using Eqs. (12) and (13), assuming the wave profile is not going to overturn or break at the next time step.

3) The wave elevation $\zeta^L(x, y, t)$ is obtained by using Eqs. (3) and (4), after correcting velocities of the fluid markers (see below). The correction of the free surface profile should be done after applying Eqs. (3) and (4), because underlying coordinates are moving with the disturbance on the free surface.

4) We linearly combine these two free surface profiles using a user-defined function γ . A possible set of the functions and parameters is given as,

$$\zeta = [1 - \gamma(x, y, t)] \zeta^E + \gamma(x, y, t) \zeta^L$$

$$\gamma(x, y, t) = \begin{cases} 1 & (x, y) \in S^L \\ \gamma \in (0, 1) & (x, y) \in S^T \\ 0 & (x, y) \in S^E \end{cases} \quad (15)$$

where S^L is the part of the free surface region considered as fully Lagrangian, S^E the remaining Eulerian region, and S^T the transition from S^L to S^E , which should connect S^L and S^E with gradual tapering. For example, these three regions (S^L , S^T , and S^E) may be of elliptical shape for an advancing pressure patch as shown in the next section. Given the problem definition for an advancing disturbance and the particular grid system, one can usually define an appropriate shape for the three zones (S^L , S^T , and S^E), for which the numerical solution will converge, with respect to their zonal shapes.

According to the Eqs. (15), the wave height function must be single-valued in the transition and Eulerian zones. When the waves are of plunger type in a particular area of the Lagrangian zone, there will be no numerical instability using this combined method, until complete overturning occurs. The Eulerian zone can be replaced by a pseudo-Lagrangian zone S^P , in case one would use instead the pseudo-Lagrangian updating method in the outer region, such as done in the work of Sung and Grilli (2005).

In this work, as we ultimately aim at predicting wave resistance for very fast vessels with air cushions, in which generated waves will break, we also need to have an efficient algorithm for absorbing wave energy and prevent wave breaking, say, near the ship stern. This aspect is tested in our simulations of waves caused by a pressure patch, and we combine our wave energy absorption scheme with a pseudo-Lagrangian method rather than the Eulerian method.

SOLUTION METHODOLOGY

High Order Boundary Element Method

The governing Eq. (1), with time-dependent nonlinear boundary conditions, is solved using the higher order 3D-FNPF-BEM model of Grilli et al. (2000, 2001), expressed for a moving disturbance problem. These references should be consulted for the numerical details of the method. The main aspects of the higher order BEM are given below.

Green's second identity transforms Eq. (1) into the BIE,

$$\alpha(\bar{x}_i)\Phi(\bar{x}_i) = \int_{\Gamma} \left[\frac{\partial \Phi}{\partial n}(\bar{x})G(\bar{x}, \bar{x}_i) - \Phi(\bar{x}) \frac{\partial G}{\partial n}(\bar{x}, \bar{x}_i) \right] d\Gamma \quad (16)$$

where $\alpha(\bar{x}_i)$ is the normalized exterior solid angle at point \bar{x}_i . The free-space Green's function is given by,

$$G(\bar{x}, \bar{x}_i) = \frac{1}{4\pi r} \quad \text{with} \quad \frac{\partial G}{\partial n}(\bar{x}, \bar{x}_i) = -\frac{1}{4\pi} \frac{\bar{r} \cdot \bar{n}}{r^3} \quad (17)$$

Where $r = |\bar{r}| = |\bar{x} - \bar{x}_i|$ is the distance from the source point \bar{x} to the field point \bar{x}_i (both on the boundary), and \bar{n} is the outward unit vector normal to the boundary at point \bar{x} .

Eqs. (16,17) are discretized and solved by a BEM, using boundary elements based on the Mid-Interval-Interpolation method (MII) (Grilli and Subramanya, 1996; Grilli et al. 2001), in which bi-cubic approximations of the free surface geometry and unknowns are expressed in 4 by 4 node sliding elements, of which only one quadrilateral (usually the central one) is used in the integrations. A curvilinear transformation is applied to express equations onto a reference element (Fig. 1). The numerical integration for source and doublet influence coefficients is carried out following the work of Grilli et al. (2001): (1) regular integrals are calculated by a bi-directional Gauss-Legendre quadrature method; (2) weakly singular integrals, where the denominator of the integrand tends to zero at a specific node point on the corresponding element, are handled by using a polar coordinate transformation, and then numerical integration; and (3) quasi-singular integrals, where the distance becomes very small but non-zero, are computed by using an 'adaptive integration' scheme, in which successive subdivisions of the element are made based on distance and solid angle criteria.

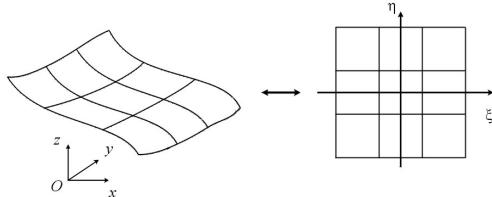


Figure 1. Sketch of 16-node cubic 3D-MII element and its corresponding reference element

Time Integration

A second order truncated Taylor series expansion is used to update the position vector \bar{R} and the velocity potential Φ on the free surface as in Grilli et al. (2001). The resulting time marching scheme for the free surface evolution and the velocity potential is as follows.

$$\bar{R}(\bar{t}_n + \delta \bar{t}_n) = \bar{R}(\bar{t}_n) + \frac{\bar{D}\bar{R}}{\bar{D}\bar{t}} \delta \bar{t}_n + \frac{\bar{D}}{\bar{D}\bar{t}} \left[\frac{\bar{D}\bar{R}}{\bar{D}\bar{t}} \right] \frac{(\delta \bar{t}_n)^2}{2} \quad (18)$$

$$\Phi(\bar{t}_n + \delta \bar{t}_n) = \Phi(\bar{t}_n) + \frac{\bar{D}\Phi}{\bar{D}\bar{t}} \delta \bar{t}_n + \frac{\bar{D}}{\bar{D}\bar{t}} \left[\frac{\bar{D}\Phi}{\bar{D}\bar{t}} \right] \frac{(\delta \bar{t}_n)^2}{2} \quad (19)$$

where $\bar{D}/\bar{D}\bar{t}$ should be chosen depending upon the type of method

used for free surface updating (i.e., Lagrangian or one of Eulerian and pseudo-Lagrangian method in the present combined method of free surface updating).

Higher-Order Spatial Derivatives

One can show that the second-order Lagrangian and pseudo-Lagrangian time derivatives in Eqs. (3) and (4), (12) and (13), respectively, can be expressed as a function of first- and second-order spatial derivatives: $\{\Phi_s, \Phi_m, \Phi_n, \Phi_{ss}, \Phi_{sm}, \Phi_{mm}, \Phi_{ns}, \Phi_{nm}\}$, and geometric quantities, where $(\bar{s}, \bar{m}, \bar{n})$ denotes an orthogonal curvilinear coordinate system on the boundary. Tangential derivatives are calculated on the boundary in a 5×5 sliding element (Grilli et al., 2001). It is also noted that Fochesato et al. (2005) recently provided more detailed and improved formulations of tangential derivatives for the model, which are used in the present applications.

NUMERICAL RESULTS

We validate the proposed combined updating methodology, by computing nonlinear waves and wave resistance caused by a moving pressure patch on the free surface. This problem has been studied earlier using theoretical or numerical methods, in relation to the design of conventional Air-Cushion Vehicles (ACVs) (e.g., Doctors and Sharma, 1972; Wyatt, 2000; Sung and Grilli, 2005).

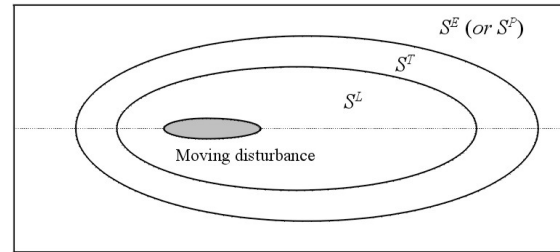


Figure 2. Definition of each free surface zone, for the combined method of free surface updating: Lagrangian (S^L), transition (S^T), Eulerian (S^E), or Pseudo-Lagrangian (S^P) zones.

Table 1. Parameters of elliptical shapes for Lagrangian and transition zones, for the present test cases

Case Number	C1	C2	C3	C4
Dimensions				
Length of major axis of S^L 's ellipse	2.0	3.0	4.5	6.5
Length of minor axis of S^L 's ellipse	1.0	2.0	3.0	3.0
Length of minor axis of S^T 's ellipse	2.5	5.0	7.5	9.5
Length of minor axis of S^T 's ellipse	1.5	3.0	4.5	4.5
Coordinates of center of ellipses	(8,0)	(8,0)	(8,0)	(10,0)

Before proceeding to compute numerical results, we further detail features of the three zones of free surface time updating used in computations, namely, Lagrangian (S^L), Transition (S^T), and Eulerian zones (S^E). Figure 2 shows a schematic for the three zones, where elliptical shapes have been used for the border of each zone. [Note, in principle, any other shape could be used depending upon the problem and areas of interest.] We solve four different test cases C1-C4, which

differ in the size of each region used for free surface time updating (Table 1). Of the four cases, C4 has the largest region where full Lagrangian updating is specified and, hence, is defined as our reference case. Numerical results are first compared between cases and later with earlier results obtained elsewhere.

As in Doctors and Sharma (1972), we define the theoretical shape of the pressure patch as,

$$p_a = M(t) \frac{p_0}{4} [\tanh \alpha(x' - x_0 + a) - \tanh \alpha(x' - x_0 - a)] \times [\tanh \beta(y - y_0 + b) - \tanh \beta(y - y_0 - b)] \quad (20)$$

in which a time ramp-up function $M(t)$ is used for initializing time-domain simulations.

Numerical results are normalized by setting $2a = 1.0$, $g = 1.0$, and $\rho = 1.0$. The relationship between dimensional and non-dimensional variables is,

$$(\hat{x}, \hat{y}, \hat{z}) = \frac{1}{L}(x, y, z), \hat{t} = \sqrt{\frac{g}{L}}t, \hat{\Phi} = \frac{\Phi}{L\sqrt{gL}}, \hat{p} = \frac{p}{\rho g L} \quad (21)$$

$$\hat{x}' = \hat{x} - \int_0^{\hat{t}} \frac{U_B(\tau)}{\sqrt{gL}} d\tau \quad (22)$$

where L is a characteristic length of the problem, $U_B(t)$ denotes the traveling velocity of the pressure patch, which is specified and normalized in this paper as,

$$\hat{U}_B(\hat{t}) = \frac{\hat{U}_B^{\max}}{2} \left\{ 1 - \cos \frac{\pi \hat{t}}{\hat{T}_m} \right\} \quad (23)$$

for $\hat{t} \leq \hat{T}_m$, and $\hat{U}_B(\hat{t}) = \hat{U}_B^{\max}$ for later times $\hat{t} > \hat{T}_m$. Herein, \hat{T}_m is the normalized time constant and $\hat{U}_B^{\max} = U_B^{\max} / \sqrt{gL}$ is the normalized maximum velocity at the steady state. A ramp-up function such as in Eq. (23) can be used for $M(t)$.

Finally, wave resistance to the motion of the disturbance is obtained as,

$$R_w = - \int_{S_{AC}} p n_x dS \quad (24)$$

where S_{AC} denotes the air-cushion surface area. This physical quantity is made dimensionless as, $R_c = (R_w / W)(\rho g a / p_0)$, where W is the weight supported by the pressure patch ($W = 4 \rho g a b$ for the present test problem).

As detailed above, a combined methodology for the free surface updating is developed, by using the conventional Lagrangian and pseudo-Lagrangian updating algorithms proposed by Sung and Grilli (2005) to solve the problem in a coordinate system traveling at the instantaneous velocity of the moving disturbance. Here we model surface waves generated by a disturbance accelerating from a state of rest to a steady state. No flow boundary conditions are applied on the downstream, upstream, and sidewall boundaries of the domain, which move at the same speed as the pressure patch. An absorbing pressure is specified over narrow strips of the free surface near the upstream boundary, in order to prevent the growth of small saw-tooth instabilities that could be created due to the enhancement of small numerical errors by the relative fluid flow (Sung and Grilli, 2005). Grid point clustering is prevented on the free surface by regridding nodes at every time step in the simulations.

Unless otherwise noted, we specify the following parameters for the pressure patch problems: $L = 2a$, $\hat{p}_0 = 0.025$, $b/a = 0.5$, $\alpha a = \beta a = 5$, $\hat{U}_B^{\max} = -1$. The computational domain is 18 dimensionless units long and 10 wide, and there are 81 and 15 node

points in x and y directions, respectively, yielding an initial grid size about 0.22 unit in each direction. The water depth is $\hat{d} = 1$ (finite-depth case). The time step and the time constant are kept constant at $\delta \hat{t} = 0.05$ and $\hat{T}_m = 2.0$, throughout the present simulations.

Figure 3 shows time histories of the relative difference between wave resistance computed as a function of time for cases C1-C3 and the reference case C4. Results are normalized by the steady-state value of the wave resistance for case C4. We see that results converge to those of case C4 as the area of the Lagrangian zone (S^L) is increased. Case C4 thus can be regarded as a case with an accurate solution in the full Lagrangian zone. In this respect, case C3 could probably be used as well, as differences with case C4 are insignificant.

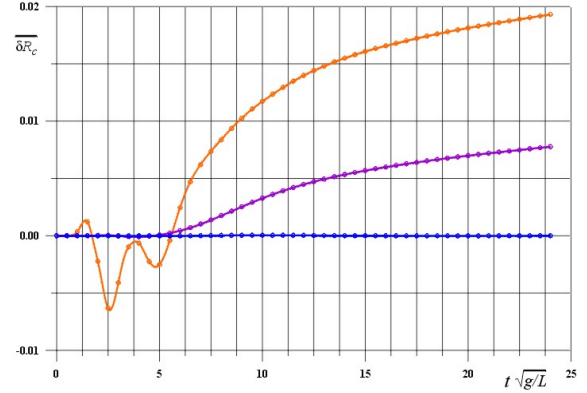
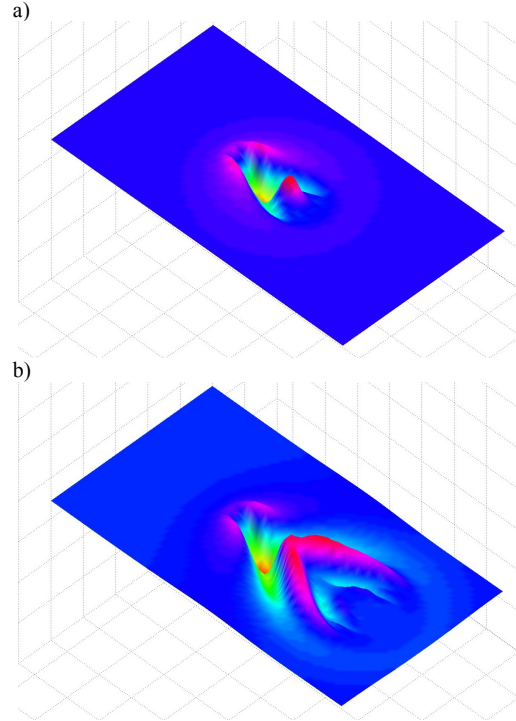


Figure 3. Effect of the size of various time-updating zones (Table 1) on total wave resistance. Relative difference with case C4 is plotted, by normalizing with the steady-state value of R_c for case C4 : (—) case C1, (—) case C2, and (—) case C3.



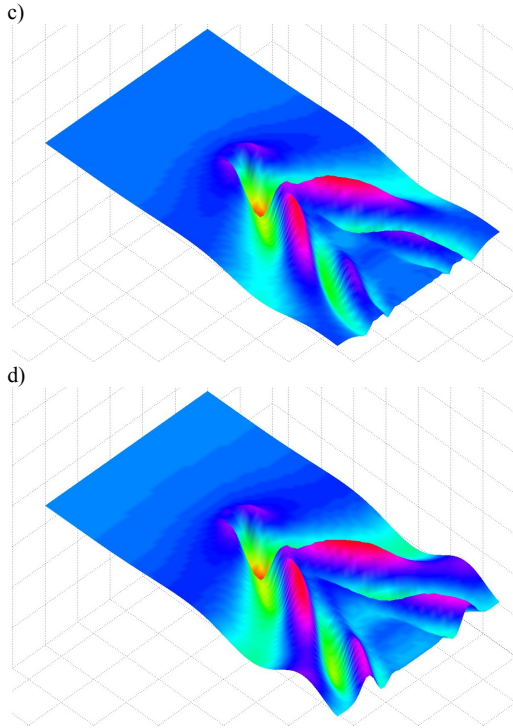


Figure 4. Free surface evolution of the advancing pressure patch problem computed using the combined time updating method, with zones of case C4 (Table 1), at $\hat{t} =$ (a) 4, (b) 8, (c) 12, (d) 16.

Figure 4 shows the time evolution of free surface waves around the traveling pressure patch for case C4. Figure 5 compares the wave resistance coefficient R_c computed with the: (i) full Lagrangian, (ii) pseudo-Lagrangian, and (iii) the present combined updating method (the latter with zones of Case C4). In each case, nonlinear time-domain simulations are performed in the same size computational domain, with the same grid system. The agreement is quite good after quasi-steady state is reached at $\hat{t} = 12 \sim 13$. The predicted values of the steady-state wave resistance are: (i) 0.971 (full-Lagrangian updating), (ii) 0.970 (pseudo-Lagrangian updating), (iii) 0.986 (the present combined method). For sake of comparison, linear wave theory yields 1.041 (Doctors and Sharma, 1972). In the Lagrangian updating, a fixed domain is used and, hence, the pressure patch eventually approaches the upstream boundary, which forces us to stop computations; also, the downstream vertical surface causes reflection and fluctuations in the computed R_w value at larger times. The pseudo-Lagrangian method is that used in Sung and Grilli's (2005) earlier results. Hence, it can be concluded that the present numerical approach, with a new combined free surface updating methodology, provides accurate and efficient results (in the sense that a much shorter domain can be used than with the full Lagrangian method, while retaining the advantages of the Lagrangian updating near the moving disturbance).

In order to check the global accuracy of the present numerical method, we compute time histories of total volume, kinetic, potential, and total energy. After computations have reached steady-state, the maximum relative error on the total volume of the computational domain is less than 0.006% (Fig. 6). At the same time, Figure 7 shows that the total energy becomes constant after reaching steady state, with nearly equal partition of kinetic and potential energy.

Figure 8 shows the steady-state free surface wave patterns obtained using the conventional full Lagrangian updating method, the pseudo-Lagrangian method of Sung and Grilli (2005), and the newly proposed combined method. In the first case, significant reflection occurs at the downstream boundary and fluctuations can also be seen at the upstream free surface boundary. These fluctuations do not occur in the pseudo-Lagrangian and the present updating methods. It is also noted that, with the full Lagrangian updating method, an open boundary condition was specified on the downstream boundary of the earth-fixed computation domain, as a pressure sensitive "snake absorbing piston wave-maker" (Brandini and Grilli, 2001).

Figure 9 shows the variation of the wave resistance coefficient computed as a function of the pressure patch speed, by using the present combined method with zones of Case 4. The faster the pressure patch moves, the earlier the wave resistance coefficient reaches steady-state, and the smaller it is.

The steady-state values of wave resistance coefficients in Figure 9 are compared in Figure 10 with those obtained by other free surface updating methods and linear theory (Doctors and Sharma, 1972). We see that all of the nonlinear methods yield smaller wave resistance results than the linear method. Moreover, the present combined method of free surface updating gives slightly smaller values of wave resistance than other free surface updating methods.

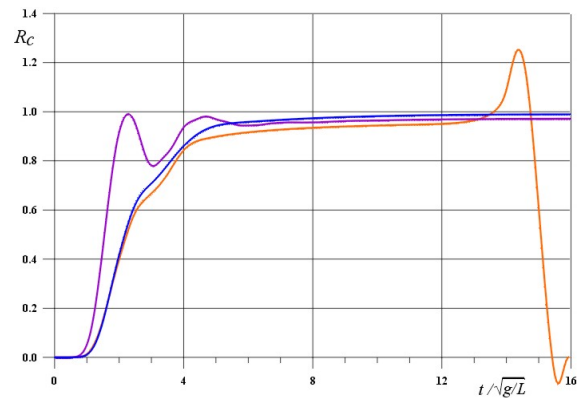


Figure 5. Time history of wave resistance coefficient for the traveling pressure patch with updating: (—) full Lagrangian, (—) pseudo-Lagrangian, and (—) combined, with zones of Case C4.

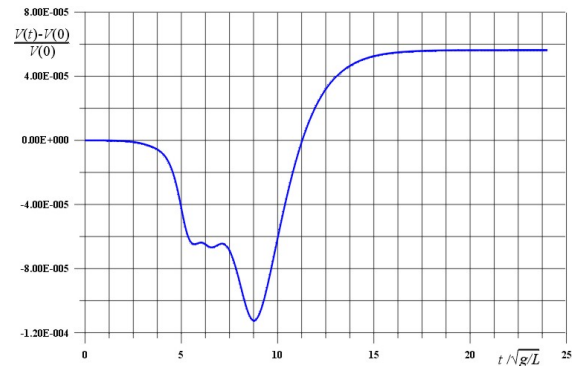


Figure 6. Mass conservation of computational domain, for traveling pressure patch with the present combined update and zones of case C4.

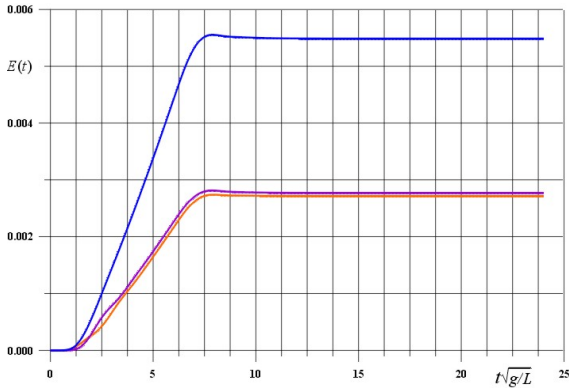
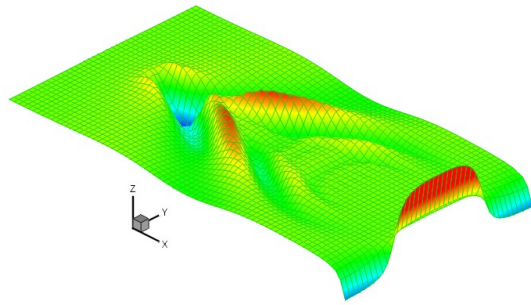
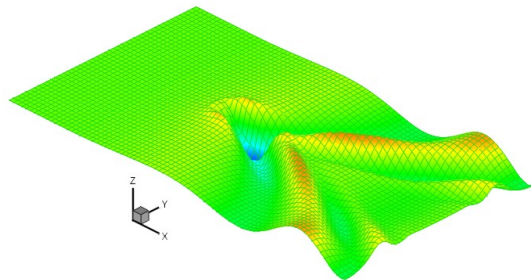


Figure 7. Wave energy for traveling pressure patch, with the present combined updating methods and zones of case C4 (same case as in Fig. 6): (—) kinetic energy ($K.E.$), (—) potential energy ($P.E.$), and (—) total energy ($T.E. = P.E. + K.E.$).

(a)



(b)



(c)

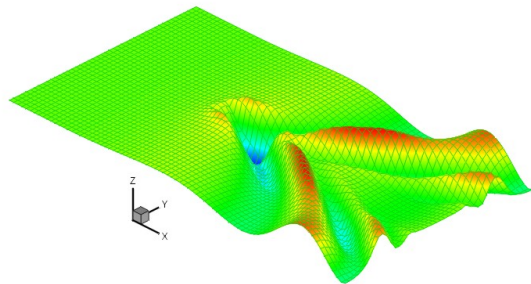


Figure 8. Comparison of steady-state free surface profiles (same case as in Fig. 5) as a function of updating method: (a) full Lagrangian, (b) pseudo-Lagrangian, and (c) combined (zones of Case C4).

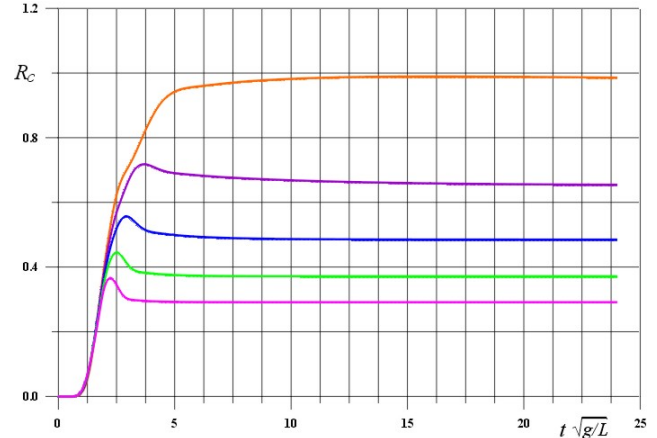


Figure 9. Variation of wave resistance coefficient as a function of pressure patch speed, with the present combined updating method and zones of case C4: (—) $\hat{U}_B^{\max} = -1.00$, (—) $\hat{U}_B^{\max} = -1.25$, (—) $\hat{U}_B^{\max} = -1.50$, (—) $\hat{U}_B^{\max} = -1.75$, and (—) $\hat{U}_B^{\max} = -2.00$.

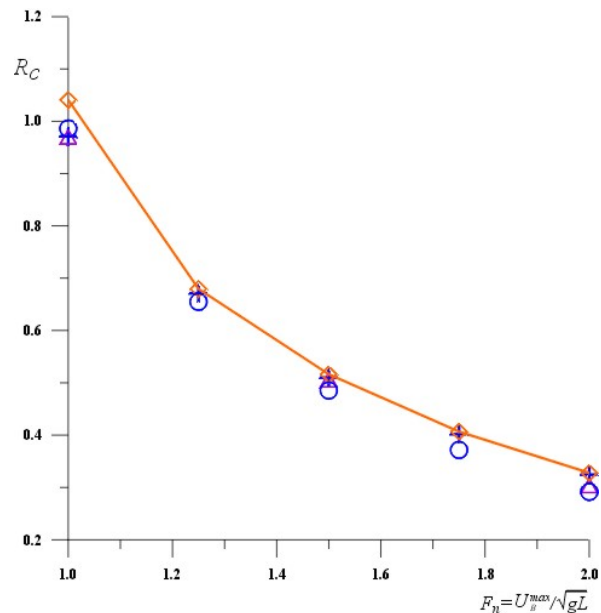


Figure 10. Comparison of the wave resistance coefficient computed with the: (O) combined updating method with zones of case C4, (Δ) full Lagrangian updating, (+) pseudo-Lagrangian updating (Sung and Grilli, 2005), and (—) linear theory (Doctors and Sharma, 1972).

It is finally noted that, Parau and Vanden-Broeck (2002) developed a steady state solution that also applies to a moving pressure patch problem. Here, however, we ultimately aim at simulating the surface flow around a fast moving disturbance, where breaking waves might occur and have to be resolved in some local areas; hence, we needed to develop an unsteady solution in which a time marching scheme is used to advance the solution in time.

CONCLUSIONS

We developed and validated a new combined methodology for updating the free surface in time in a 3D-FNPN-BEM model (Grilli et al. 2000, 2001). Numerical results obtained for a traveling pressure patch problem show that the new proposed method of the paper is not only more advantageous to use for this problem, but also as accurate as the conventional full Lagrangian and pseudo-Lagrangian methods used earlier by Sung and Grilli (2005).

ACKNOWLEDGEMENTS

Authors acknowledge support from a grant from Ocean Dynamics Inc., Wickford, RI, USA, awarded to the University of Rhode Island. The first author's work was partially supported by the Post-doctoral Fellowship Program of Korea Science & Engineering Foundation (KOSEF), and by the principal R&D program of KORDI: "Development of Safety Evaluation Technologies for Marine Structure in Disastrous Ocean Waves" granted by Korea Research Council of Public Science and Technology.

REFERENCES

- Beck, R.F. (1999), "Fully nonlinear water wave computations using a desingularized Euler-Lagrange time domain approach, In *Nonlinear Water Wave Interaction*," O. Mahrenholtz & M. Markiewicz, Eds., *Advances in Fluid Mechanics Series*, WIT Press, 1-58.
- Beck, R. F. and A. M. Reed (2001), "Modern computational methods for ships in a seaway," *SNAME Transactions*, 109, 1-51.
- Dawson, C. W. (1977), "A practical computer method for solving ship-wave problems," *Proc. 2nd Intl. Conf. Num. Ship Hydro.*, Berkley, CA, 30-38.
- Doctors, L. J. and S. D. Sharma (1972), "The Wave Resistance of an Air-Cushion Vehicle in Steady and Accelerated Motion," *Journal of Ship Research*, 16, 248-260.
- Dommermuth, D.G., Yue, D.K.P., Lin, W.M., Rapp, R.J., Chan, E.S. and Melville, W.K. (1988), "Deep-water Plunging Breakers: A Comparison Between Potential Theory and Experiments," *J. Fluid Mech.*, 184, 267-288.
- Fochesato C., Grilli, S. and Guyenne P. (2005), "Note on non-orthogonality of local curvilinear co-ordinates in a three-dimensional boundary element method," *International Journal for Numerical Methods in Fluids*, 48, 305-324.
- Grilli, S.T., P. Guyenne, & F. Dias (2000), "Modeling of overturning waves over arbitrary bottom in a 3D numerical wave tank," *Proc. 10th Int. Offshore and Polar Eng. Conf.*, 3, 221-228.
- Grilli, S.T., P. Guyenne and F. Dias (2001), "A fully non-linear model for three-dimensional overturning waves over an arbitrary bottom," *International Journal for Numerical Methods in Fluids*, 35, 829-867.
- Grilli, S. T. and J. Horrillo (1997), "Numerical generation and absorption of fully nonlinear periodic waves," *Journal of Engineering Mechanics*, 123, 1060-1069.
- Grilli, S.T., Svendsen, I.A. and Subramanya, R. (1997), "Breaking Criterion and Characteristics for Solitary Waves on Slopes," *J. Waterway Port Coastal and Ocean Engineering*, 123(3), 102-112.
- Hess J. L. and A. M. O. Smith (1964), "Calculation of nonlinear potential flow about arbitrary three-dimensional bodies," *J. Ship Res.* 8(2), 22-44.
- Hino, T. (1989), "Computations of a free surface flow around an advancing ship by the Navier-Stokes equations," *Proc. 5th Int. Conf. Num. Ship Hydro.*, 103-117.
- Huang, Y. & P. D. Sclavounos (1998), "Nonlinear ship motions," *Journal of Ship Research*, 42(2), 120-130.
- Jensen, G., V. Bertram and H. Söding (1989), "Ship wave-resistance computations," *Proceedings of the 5th International Conference on Numerical Ship Hydrodynamics*, Hiroshima, Japan, 593-606.
- Liu Y., M. Xue & D. K. P. Yue 2001, Computations of fully nonlinear three-dimensional wave-wave and wave-body interactions. Part 2. Nonlinear waves and forces on a body, *Journal of Fluid Mechanics*, 438, 41-66.
- Longuet-Higgins, M.S. and Cokelet, E.D. (1976), "The Deformation of Steep Surface Waves on Water, I. A Numerical Method of Computations," *Proc. Roy. Soc. London*, 1976, Ser. A, 350, 1-26.
- Muscari, R. and A. Di Mascio (2004), "Numerical modeling of breaking waves generated by a ship's hull," *J. Marine Sc. And Tech.* 9, 158-170.
- Noblesse F. (2000), "Analytical representation of ship waves," *23rd Weinblum Merorial Lecture*, Hydrodynamic Directorate Technical Report NSWCCD-TR-2000/011, Naval Surface Warfare Center, Carerock Division.
- Parau, E. and Vanden-Broeck, J.-M. (2002), "Nonlinear two- and three-dimensional free surface flows due to moving disturbances," *European Journal of Mechanics - B/Fluids*, 21(6), 643-656.
- Pawloski, J. S. (1991), "A theoretical and numerical model of ship motions in heavy seas," *SNAME Transactions*, 99, 319-352.
- Raven, H.C. (1998), "Inviscid calculations of ship wave making-Capabilities, limitations, and prospects," *Poceedings of the 22nd Symposium on Ship Hydrodynamics*, Washington, D.C., 738-754.
- Saad, Y. and Schultz, M.H. 1986, GMRES: A generalized minimal residual algorithm for solving nonsymmetric linear systems, *SIAM Journal of Scientific Statistic Computation*, No. 7, 856-869.
- Sclavounos, P. D., D. C. Kring, Y. Huang, D. A. Mantzaris, S. Kim, and Y. Kim (1997), "A computational method as an advanced tool of ship hydrodynamic design," *SNAME Transactions*, 105, 375-397.
- Sung, H.G. and Grilli, S.T. (2005), "Numerical Modeling of Nonlinear Surface Waves caused by Surface Effect Ship: Dynamics and Kinematics," *Proceedings of the Fifteenth ISOPE Conference*, 124-131.
- Sung, H.G., Sa Y. Hong and Hang S. Choi (2000), "Evaluation of non-linear wave forces on a fixed body by the higher-order boundary element method," *Journal of Mechanical Engineering Science (Proceedings of the Institution of Mechanical Engineers Part C)*, 214, 825-839.
- Wehausen, J.V. (1973), "The wave resistance of ships," *Advances in Applied Mechanics*, 13, 93-245.
- Wyatt, D. C. (2000), "Development and Assessment of a Nonlinear Wave Prediction Methodology for Surface Vessels," *Journal of Ship Research*, 44(2), 96-107.